Laser-induced fluorescence and up-conversion processes in LiYF$_4$: Nd^{3+} laser crystals

M. Malinowski,* B. Jacquier, M. Bouazaoui, M. F. Joubert, and C. Linares

Universite Claude-Bernard (Lyon 1), 69622 Villeurbanne CEDEX, France

(Received 15 May 1989)

Tunable-pulsed-laser spectroscopy was used to investigate the anti-Stokes fluorescence of the Nd^{3+} ion in LiYF$_4$ crystals. On the basis of time-resolved measurements at 4.4 K, the observed fluorescence lines in the near uv and blue region (356–417 nm) were assigned to transitions from the $^4D_{3/2}$ and $^2P_{3/2}$ excited states. These emissions were examined under both one- and two-photon laser excitations. These excitation conditions, added to the time-resolved-spectroscopy technique, provide convincing arguments for a detailed description of the various high-energy Nd^{3+} states in LiYF$_4$. The dominant process leading to anti-Stokes fluorescence was attributed to an excited-state absorption from the $^4F_{3/2}(1)$ and $^4F_{5/2}$ states, which were probed by a two-color laser excitation experiment. The kinetics of deexcitation of the $^4D_{3/2}$, $^2P_{3/2}$, and $^4F_{3/2}$ states were investigated under various excitation conditions and over a wide range of temperatures. A detailed discussion emphasizes relaxation of the excited states.

I. INTRODUCTION

Studies of nonlinear processes leading to anti-Stokes fluorescence in various rare-earth (RE) compounds have generated new interest since the development of high-power dye lasers. Two important processes of this type are multiphoton absorption through a virtual intermediate quantum state and stepwise absorption with a real resonant intermediate state. In the first case the total energy of the photons must satisfy the resonance conditions exactly, while in the case of stepwise absorption, all of the excitation frequencies must be in resonance with the successive quantum transitions.[1] Two-photon absorption (TPA) has proven to be a powerful spectroscopic tool complementary to one-photon spectroscopy.[2,3] Its advantage over one-photon excitation is the possibility of exciting high-lying states without using vuv radiation, and, because of the fact that the TPA transitions are parity allowed within the $4f$ configuration of RE ions, it provides additional selectivity.

Interest in these multiphoton transitions has also been stimulated by the practical significance of high-energy R^{3+} transitions for use in anti-Stokes uv lasers, i.e., devices whose output frequency is higher than that of the pump light. Recently, Silversmith et al.[4] reported infrared laser pumping of a green Er^{3+} laser in YAlO$_3$:Er^{3+}, and Lenth et al. reported on up-conversion laser action in LiYF$_4$:Er^{3+} crystals.[5] Violet and blue cw neodymium laser action in LaF$_3$ and LiYF$_4$, respectively, have been also observed by Macfarlane et al.[6] This explains why the well known and most important neodymium activated solid-state crystalline materials such as LaF$_3$:Nd^{3+}, Y$_3$Al$_5$O$_{12}$:Nd^{3+} (YAG:Nd^{3+}), LiYF$_4$:Nd^{3+} (YLF:Nd^{3+}), and YAlO$_3$:Nd^{3+} are still intensively studied. The first observation of multiphoton effects in YAG:Nd^{3+} was reported by Danielmeyer and Blatte[7] in 1973. Kramer and Boyd[8] reported on the resonantly enhanced, three-photon absorption in YAG:Nd^{3+} lead-

ing to the strong visible fluorescence in the 400 nm region. This emission in YAG:Nd^{3+} has also been studied by Quarles et al.,[9] however, contrary to earlier results, it was interpreted as resulting from sequential two-step absorption with a real resonant intermediate level. The complex visible fluorescence spectra of Nd^{3+} ions in YAG crystals were observed by Mares et al.[10] Spectroscopic investigations of anti-Stokes emission after two-photon absorption by ion pairs in LaF$_3$:Nd^{3+} and YLF:Nd^{3+} have also been reported.[11,12] Recently, Chase and Payne[13] have obtained extensive TPA spectra for the $^4I_{9/2} \rightarrow {}^4G_{7/2}$ transitions of Nd^{3+} doped YAG and YLF crystals. Their TPA cross-section measurements were in satisfactory agreement with the developed theoretical model. In view of its role in laser applications, Nd^{3+}-doped YLF can rival YAG, and it even presents some advantages such as the infrared (IR) laser wavelength better matched to the Nd^{3+} glass amplifiers and longer lifetime of the $^4F_{3/2}$ metastable level than in YAG. Fan and Byer[14] demonstrated the possibility of using YLF:Nd^{3+} as an up-conversion laser at 411.7 nm, and Macfarlane has observed the laser action on the $^2P_{3/2}(1) \rightarrow {}^4F_{5/2}(2)$ and $^2P_{3/2}(1) \rightarrow {}^4I_{9/2}(1)$ transitions at 792.5 and 412.9 nm, respectively, in LiYF$_4$:Nd^{3+}.[15] It is also assumed that, because of the higher S_4 site symmetry of the R^{3+} ion in YLF (compared to YAG), more strictly obeyed selection rules for TP transitions will facilite the interpretation of the YLF polarized spectra.

With these objectives in mind, the detailed investigations of various up-conversion processes in YLF:Nd^{3+} have been made and are presented in this study. There is still some controversy on the detailed position of Nd^{3+} electronic levels in YLF (see, for example, Refs. 13 and 16), and very little work has been done on studying the dynamics of the excited states. So our anti-Stokes fluorescence measurements are supported by the analysis of one- and two-photon excited fluorescence spectra. The properties of a new metastable state together with the po-

sition of other high-lying states were characterized and different types of two-photon processes were identified.

II. DYNAMICS OF THE FUNDAMENTAL MECHANISMS

Selective pulsed-laser excitation together with time-resolved techniques (TRS) provides a well-suited tool for investigating the identification and relaxation of excited states of RE-doped crystals. Besides the one-photon absorption that allows us to reach directly a designated excited state, our studies are presently concerned with various two-photon absorption processes involved in the creation of anti-Stokes fluorescence. Two fundamentally different mechanisms, involving either one active ion or two (or more) RE ions, can be experimentally distinguished by several criteria such as the energy-levels diagrams of both ions, their coincidences as well as their differences, the rise and decay times of the emission, and the concentration dependence of the activator. As a consequence of the interaction between two active ions, energy transfer or cooperative phenomena result in a time-retarded fluorescence that generally exhibits rise and decay times characteristic or the excited-state lifetime (either anti-Stokes or pumping levels) involved in the processes. On the contrary, direct two-photon or excited-state absorption in one center creates instantaneously or quasiinstantaneously a population in the fluorescing state leading to the observation of an exponential anti-Stokes fluorescence decay with a time constant characteristic of the metastable excited state. It is important to note that the absence of resonance either in the up-conversion energy transfer process or in the excited-state absorption does not change the time dependence described above, in contrast to intensity variations that occur because of the probability of relaxation processes through the absorption of intermediate states. In the above considerations, we have restricted the discussion to the case where the two-color laser excitations are coincident. As a matter of fact a measurement of the anti-Stokes (AS) fluorescence intensity as a function of a delay between the two lasers producing sequential processes will image the relaxation rate towards the intermediate or fluorescing states.

One can summarize the fluorescence decay behavior expected for various one- and two-ion processes as it has been well established in the literature using the rate equation model:

(i) One-ion process:

$$I_{AS}(t) \simeq n_a(t) = N_a \exp(-W_a t) , \tag{1}$$

where N_a and W_a are the initial population and the deexcitation probability of the anti-Stokes fluorescing state, respectively.

(ii) The up-conversion energy transfer process requires solving a bilinear equation that only possesses an analytical solution at low-excitation densities. Then, the anti-Stokes fluorescence intensity is described by the following expression:

$$I_{AS}(t) \simeq n_a(t) = \alpha_a N_a \exp(-W_a t) + \alpha N_p^2 \exp(-2W_p t) \tag{2}$$

with

$$\alpha_a = 1 - \frac{N_p^2}{N_a} \alpha, \quad \alpha = \frac{1}{2} \frac{W_T}{W_a - 2W_p} ,$$

where N_p and W_p are the initial population and the deexcitation probability of the pumping state, respectively, and W_T is a coefficient including the energy transfer rate. Finally, using the time-resolved fluorescence technique, as well as the fluorescence decay analysis, it should be possible to interpret the feeding of various states involved in the up-conversion processes. Furthermore, the sensitizer concentration dependence can resolve possible ambiguities.

III. EXPERIMENTAL METHODS

Two single-crystal samples of $LiYF_4$ doped with Nd^{3+} in nominal concentration of 0.1% and 3% were used for our measurements. Both crystals were grown by the Bridgman method by the Laboratoire d'Electronique de Technologie et d'Instrumentation (Grenoble, France). The crystal structure is tetragonal (sheelite $CaWO_4$) space group C_{4h}, and the site symmetry of the Nd^{3+} ion is S_4. The crystals were oriented by x-ray technique and then cut and polished to the form of cubes several mm in size.

For absorption measurements in the range from 180 to 800 nm, a Cary 2300 Varian spectrophotometer equipped with a continuous flow He refrigerator was used. For emission measurements a liquid He cryostat with a heating gas system allowing the temperature to vary from 1.6 to 300 K was used. A frequency-doubled Quantel model 481 YAG:Nd^{3+} laser followed by a three-stage amplifier dye laser (pulsewidth 15 ns, linewidth 0.1 cm^{-1}) served as the excitation source in the visible range. For a tunable excitation in the near uv region the second harmonic of a dye laser was used. In our two laser experiments the doubled YAG:Nd^{3+} ($\lambda = 532$ nm) laser pumped two identical small dye lasers, each giving pulses of about 10 ns width, 0.1 cm^{-1} bandwidth, and up to 500 μJ in energy. The alignment and focusing of the two laser beams was verified with a system developed using two perpendicular razor blades.

To select the polarization for the various experiments a Soleil-Babinet compensator together with a calcite polarizer was used. The crystal was oriented so its c axis was perpendicular to the direction of beam propagation. Fluorescence was analyzed by a 1 m Hilger and Watts monochromator with the 8 Å/mm resolution followed by EMI 9789 or RCA AsGa photomultiplier tubes. The signal was processed by an Ortec photon counting system. The experimental setup was controlled by the Tektronix 4051 graphics computer. For the two-color experiment a PC computer manages the wavelengths of the dyes and the fluorescence signal is processed by a Lecroy multichannel analyzer. The decay curves were recorded by the Canberra 35+ multichannel analyzer with 200 ns per channel resolution.

IV. RESULTS

A. One-photon excitation

As preliminary measurements the one-photon excited spectra of YLF:Nd^{3+} have been investigated at 4.4 K.
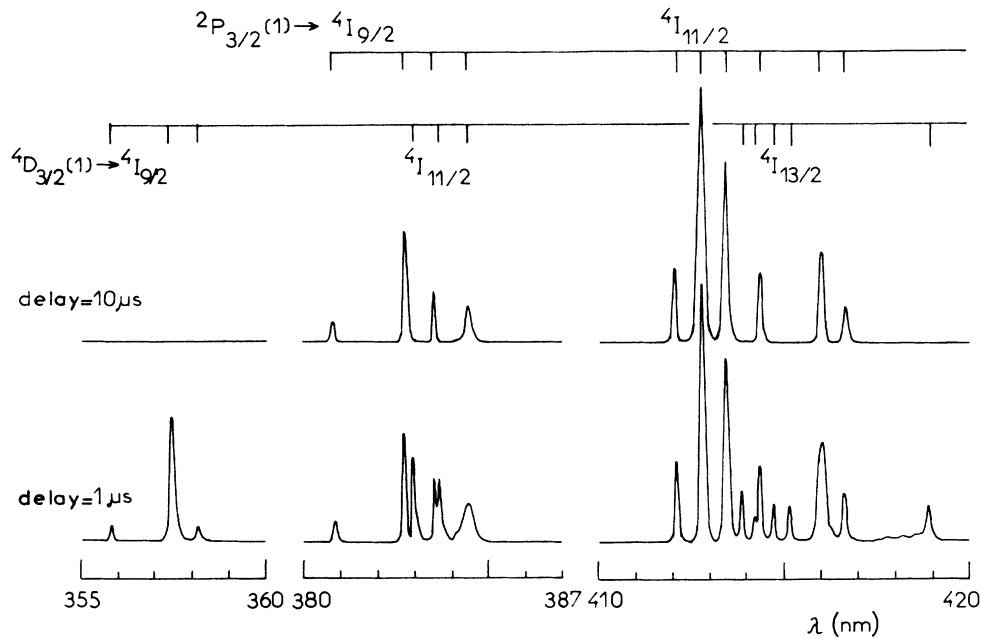
FIG 1. Fluorescence spectra of LiYF$_4$: 0.1 at. % Nd^{3+} at two times after the excitation pulse at 299.2 nm, $T=4.4$ K.

After selective excitation of one of the Stark components of the $^2D_{3/2}$ level lying at 33 426 cm^{-1}, several intense fluorescence lines of Nd^{3+} ions in the blue and near uv were observed. Because of the overlapping of these transitions, the time resolved spectroscopy (TR) was used to make a precise assignment. TR fluorescence spectra in the 350–420 nm region are shown in Fig. 1. The observed transitions were identified as originating from the

FIG. 2. Main fluorescence transitions of Nd^{3+} ions in LiYF$_4$ observed at 4.4 K (note all levels of Nd^{3+} are not shown).

$^4D_{3/2}$ and $^2P_{3/2}$ excited states to various Stark components of the ^4I_J multiplets.

The $^4D_{3/2}$ and $^2P_{3/2}$ fluorescence lifetimes measured at 4.4 K were found to be about 1.3 μs and 37 μs, respectively, in the 3 at. % Nd^{3+} doped sample and 1.3 μs and 50 μs, respectively, in the 0.1 at. % Nd^{3+} sample. The $^4D_{3/2}$ and $^2P_{3/2}$ fluorescence have been observed up to 600 K. The near ir transitions originating mostly from the $^4F_{3/2}$ state were also measured. For the 0.1 at. % Nd^{3+} sample the low-temperature $^4F_{3/2}$ lifetime of 670 μs was found. The experimentally determined positions of the YLF:Nd^{3+} emission lines at 4.4 K are presented in Fig. 2 and are also tabulated in Table I.

Because the first goal of our investigation was to study the TPA transitions, the $^4I_{9/2}(1)\rightarrow{}^2H(1)_{9/2}$ transition satisfying the $\Delta L,\Delta J < 2$ (Ref. 17) selection rules was chosen. This type of experiment requires the detailed knowledge of the energy level positions around the one-photon energy. Thus, the polarized, $\Pi(E\|\hat{c})\sigma(E\perp\hat{c})$, excitation spectra of the ir $^4F_{3/2}\rightarrow{}^4I_{9/2}$ fluorescence have been registered when scanning the laser wavelength around the $^2H(2)_{11/2}$ and $^4G_{5/2}+{}^2G(1)_{7/2}$ absorption lines and are presented in Fig. 3. It could be seen that the transitions are strongly polarized: in the dilute YLF: 0.1 at. % Nd^{3+} sample the smallest linewidth of 0.17 cm^{-1} was measured for the $^4I_{9/2}(1)\rightarrow{}^2H(2)_{11/2}$ transition. For the $^4I_{9/2}(1)\rightarrow{}^4G_{5/2}(1)$ transition we retrieve the satellite line structure reported earlier by Barthem et al.[18] In the 3 at. % Nd sample, however, the lines were much broader and several intense additional lines were clearly observed. Thus, to avoid any energy transfer processes or nonequivalent-ion-sites effects most of our further experiments have been performed on the 0.1 at. % Nd^{3+} doped YLF crystal.

The low-temperature excitation spectra recorded in the

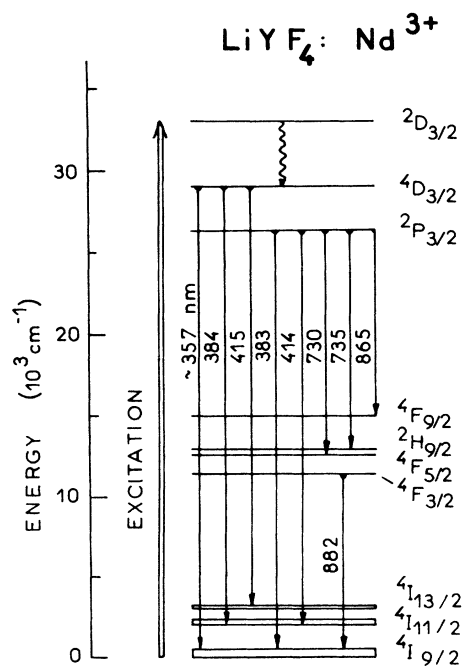TABLE I. Fluorescence transitions for $LiYF_4$: Nd^{3+} at 4.4 K.

Transition	λ (Å)	E (cm^{-1})
$^4D_{3/2}(1)\rightarrow^4I_{9/2}$	3558.0	28 106
	3574.6	27 975
	3581.5	27 921
$^2P_{3/2}(1)\rightarrow^4I_{9/2}$	3808.2	26 259
	3827.3	26 128
	3835.2	26 074
	3844.4	26 012
$^4D_{3/2}(1)\rightarrow^4I_{11/2}$	3829.8	26 111
	3836.2	26 067.5
	3841.4	26 032
$^2P_{3/2}(1)\rightarrow^4I_{11/2}$	4121.4	24 264
	4128.7	24 220
	4134.8	24 185
	4143.7	24 133
	4160.6	24 035
	4167.5	23 995
$^4D_{3/2}(1)\rightarrow^4I_{13/2}$	4138.8	24 161[a]
	4142.1	24 142[a]
	4147.3	24 112[a]
	4152.1	24 084[a]
$^2P_{3/2}(1)\rightarrow^4F_{5/2}$	7285.6	13 726
	7291.0	13 716
$^2P_{3/2}(1)\rightarrow^2H_{9/2}$	7333.5	13 636
	7342.4	13 619.5
	7354.7	13 597
	7387.4	13 536
	7431.2	13 457
$^4F_{3/2}(1)\rightarrow^4I_{9/2}$	8663.3	11 543
	8762.7	11 412
	8804.4	11 358
	8852.7	11 296
$^2P_{3/2}(1)\rightarrow^4F_{9/2}$	8685.4	11 513.5
	8708.2	11 483
$^4F_{3/2}(1)\rightarrow^4I_{9/2}$	8663.3	11 543
	8762.7	11 412
	8804.5	11 358
	8852.8	11 296
	9074.4	11 020

[a]In 0.1 at. % Nd^{3+}: $LiYF_4$ only.

298–650 nm range, together with our absorption and fluorescence measurements, resulted in the detailed energy-level scheme presented in Table II. In the case when the polarized spectra were recorded the symmetry properties of the energy levels were determined and the levels are labeled by the irreducible representations of the S_4 group, $\Gamma_{5,6}$ and $\Gamma_{7,8}$.[19]

B. Two-photon spectra

The TPA of the $^4I_{9/2}(1)\rightarrow^2H(1)_{9/2}$ transitions of Nd^{3+} was examined by monitoring the uv $^4D_{3/2}$ emission when scanning the laser excitation frequency in the vicinity of one-half the examined transition energy. Results of these two identical photon experiments, together with the

one-photon excitation spectra of the $^4I_{9/2}\rightarrow^2H(1)_{9/2}$ transition, are shown in Fig. 4. Clearly, the TPA spectrum is composed of only one intense, sharp line at 6038 Å (16 563 cm^{-1}); its position, however, does not agree with any of the tabulated $^2H(1)_{9/2}$ energies. This experiment has been performed with the same result under Π and σ polarized excitation. In the 3 at. % doped sample some very weak features around 6000 Å could be observed in σ polarization (see inset in Fig. 3). The quadratic dependence of the uv fluorescence on excitation intensity, determined by computer integration of the emission bands, was found and is shown in Fig. 5. Similar behavior was observed while monitoring the $^4F_{3/2}$ emission.

With our two-laser experiments one of the lasers was detuned by several cm^{-1} from the 16 563 cm^{-1} frequency and the second was set to match the resonance, 33 126 cm^{-1} conditions. In these two different photon excitation experiments, however, no $^4D_{3/2}$ nor $^2P_{3/2}$ and $^4F_{3/2}$ fluorescences were observed. This suggests that some processes other than TPA with a virtual intermediate level is responsible for the uv emission and that the 6038 Å excitation is in resonance with some real electronic Nd^{3+} level.

It has been also found that the uv fluorescence could be generated after direct excitation of any of the Stark components of the $^2H(2)_{11/2}$ or $^3G_{5/2}$ states (see also Fig. 3). Several two-color laser experiments have been performed when one of the lasers was fixed at 6038 Å, and the second was tuned to only of the $^2H(2)_{11/2}$ absorption lines, see Table II. With only the first laser (6038 Å) turned on, the measured uv signal was of 35 counts/sec intensity. With only the second laser operating the uv signal was of 70 counts/s and 750 counts/s intensity, respectively, for 6229 Å (16 055 cm^{-1}) and 6196 Å (16 138 cm^{-1}) absorption. With both lasers operating simultaneously the uv signal was of 2200 counts/s and 6000 counts/s intensity, respectively.

C. Lifetime measurements

It is also interesting to compare the presented intensity results with those obtained from our lifetime measurements. In all of the two-photon experiments the uv $^4D_{3/2}$ fluorescence at about 3580 Å was used as a probe. In Fig. 6 the one-photon 2992 Å (33 426 cm^{-1}) excited $^4F_{3/2}$ fluorescence decay curves in the 0.1 at. % Nd^{3+} doped $LiYF_4$ crystal are presented. In the lower part of the figure, the $^4F_{3/2}$ decay for short times after the laser pulse is shown. In Fig. 7 the $^4D_{3/2}$ and $^2P_{3/2}$ fluorescence decay curves after 2992 Å excitation are presented. It was observed that, in the investigated crystals, the $^4D_{3/2}$ decay is independent of active ion concentration, whereas the $^2P_{3/2}$ emission becomes shorter and nonexponential in the 3 at. % Nd^{3+} doped sample.

It was also seen that the 6038 Å excitation (in both one- and two-laser pumping schemes as well as in direct excitation of one of the $^2H_{11/2}$ Stark levels) results in a $^4D_{3/2}$ decay with no observable rise time and a decay constant unchanged from that under direct uv excitation. In contrast, the buildup of the $^4F_{3/2}$ fluorescence is slow, with a characteristic time of about 3 μs. Figure 8 shows
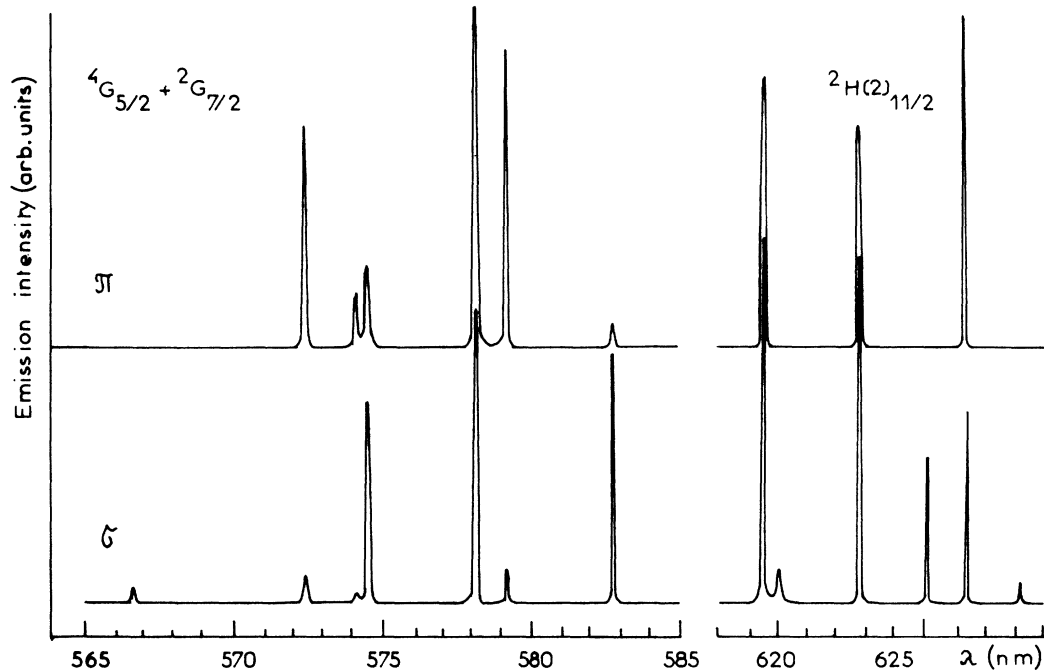
FIG. 3. One-photon excitation spectra of the $^4I_{9/2}(1)\rightarrow{}^4G_{5/2}+{}^2G_{7/2}+{}^2H(2)_{11/2}$ transitions of 0.1 at. % Nd^{3+} doped $LiYF_4$ measured at 4.4 K for σ and π polarizations of pumping radiation. The Nd^{3+} $^4F_{3/2}\rightarrow{}^4I_{9/2}$ emission was monitored while the laser was scanned across the absorption lines.

the results of measuring the $^4D_{3/2}$ and $^2P_{3/2}$ fluorescence lifetimes as a function of temperature. We found that up to 300 K the uv fluorescence lifetime is independent of temperature, whereas a decrease of the blue $^2P_{3/2}$ emission lifetime was observed for temperatures higher than about 200 K. For temperatures higher than 300 K the uv $^4D_{3/2}$ fluorescence decay time exhibits a double exponential behavior as a result of a phonon annihilation process from the $^2P_{3/2}$ state.

V. DISCUSSION

Fluorescence and absorption spectra of $YLF:Nd^{3+}$ have been studied previously;[16,20] however, we present the detailed structure of the short wavelength fluorescence together with its precise assignment. This identification has been facilitated by the large difference in the $^4D_{3/2}$ and $^2P_{3/2}$ fluorescence lifetimes, 1.3 μs and 50 μs, respectively, in the 0.1 at. % Nd^{3+} sample, which
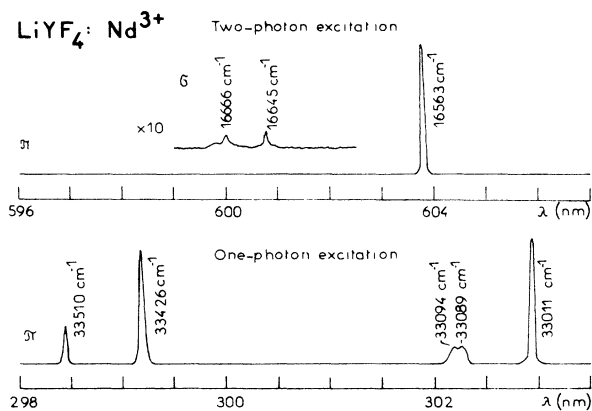

FIG. 4. One-photon excitation spectrum of the $^4D_{3/2}(1)$ fluorescence and two-photon excitation spectrum of the $^4D_{3/2}(1)$ emission in the vicinity of one-half the observed one-photon transitions of $LiYF_4$: 0.1 at. % Nd^{3+}. $T=4.4$ K.
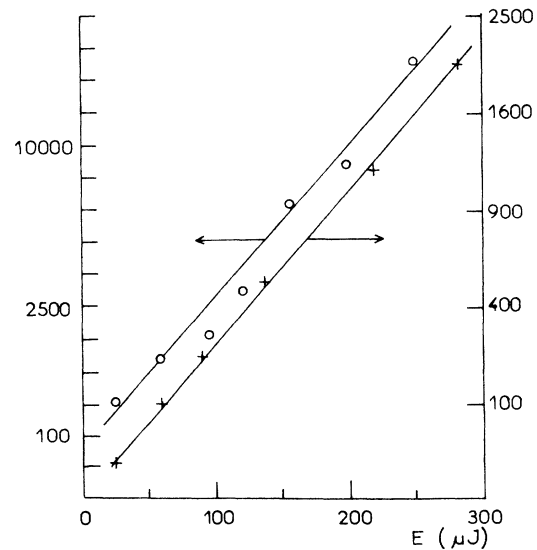

FIG. 5. uv $^4D_{3/2}(1)$ and ir $^4F_{3/2}(1)$ emissions as a function of the laser pump power at 603.8 nm. $\bigcirc$, $\int Em(ir)\,dv$ (arbitrary units); $+$, $\int Em(uv)\,dv$ (arbitrary units).

TABLE II. Experimental energy levels for LiYF$_4$: 0.1 at.% Nd^{3+} at 4.4 K. An asterisk denotes less accurate results.

Multiplet	E (cm^{-1}) (In absorption)	E (cm^{-1}) (In emission or excitation)	Γ
$^2F(2)_{7/2}$	40 000		
	39 936		
$^2F(2)_{5/2}$	38 647		
	38 477		
$^2D(2)_{3/2}$	33 515.5	33 510	
	33 431	33 426	
$^2H(1)_{9/2}$	33 104	33 094	
		33 089	
	33 025	33 011	
		32 910	
$^2L_{17/2}$	31 931		
	31 851	31 847.5	
	31 808		
		31 787	
		31 730	
	30 921.5	30 916	
	30 674		
	30 567		
	30 446		
	30 367		
	30 234		
$^2I_{11/2}$	29 381		
	29 372*		
	29 300*		
	29 202		
$^4D_{1/2}$	27 798.5		
$^4D_{5/2}$	28 578		
	28 531*		
	28 522.5		
not assigned	28 444.5		
	28 406		
	28 369		
	28 341.5		
$^4D_{3/2}$	28 220	(28 209 in 3 at.% Nd)	
	28 109.5	28 106 (28 097 in 3 at.% Nd)	
$^2P_{3/2}$	26 346		
	26 264	26 259 (26 252 in 3 at.% Nd)	
$^2G(1)_{7/2}$		17 644	$\Gamma_{7,8}$
		17 469	$\Gamma_{5,6}$
		17 414	$\Gamma_{5,6}$
		17 405	$\Gamma_{7,8}$
$^4G_{5/2}$		17 293	$\Gamma_{7,8}$
		17 265	$\Gamma_{5,6}$
		17 154	$\Gamma_{7,8}$
$^2H(2)_{11/2}$	16 141	16 138	$\Gamma_{5,6}$
		16 126	$\Gamma_{7,8}$

Multiplet	E (cm^{-1}) (In absorption)	E (cm^{-1}) (In emission or excitation)	Γ
$^2H(2)_{11/2}$	16 058	16 055	$\Gamma_{5,6}$
	16 005		
	15 997	15 995	$\Gamma_{7,8}$
	15 969	15 967	$\Gamma_{5,6}$
	15 922	15 919	$\Gamma_{7,8}$
$^4F_{9/2}$	14 951		
	14 893		
	14 880	14 776	
	14 750	14 746	
$^4S_{3/2}+$	13 661		
+	13 642		
$^4F_{7/2}$	13 524		
	13 499		
	13 496.5	13 494	
$^2H(2)_{9/2}$	12 807	12 802	
	12 734	12 730	
	12 667	12 662	
	12 645	12 639.5	
$^4F_{5/2}$	12 629.5	12 624	
	12 549		
	12 547*	12 543	
	12 539		
	12 536.5	12 533	
$^4F_{3/2}$	11 543		
$^4I_{13/2}$	4239		
	4022		
	3994		
	3965.5		
	3945		
$^4I_{11/2}$	2263		
	2224		
	2125		
	2074		
	2038.5		
	1995		
$^4I_{9/2}$	523		
	247		
	185		
	131		
	0		

made the use of the TRS technique possible and very efficient.

The fluorescence lifetime of the $^2P_{3/2}$ level, calculated from the energy gap dependence to the next lower-lying level, was found to be 83 μs. The observed dependence of the $^2P_{3/2}$ lifetime on neodymium doping concentration and its nonexponential character in the 3 at.% Nd^{3+} doped crystal suggests the presence of a cross-relaxation quenching, probably a one phonon assisted process via various intermediate states, $^4I_{11/2}$ and $^4F_{7/2}$. The position of several Stark levels, for example $^4D_{3/2}(1)$ and $^2P_{3/2}(1)$, see Table II, is also concentration dependent due to Nd^{3+} induced strains in the YLF lattice. The linewidth measurements are in good agreement with the results of Buisson et al.[12] Some weak satellite structure related to isolated ion-pair lines have been observed in
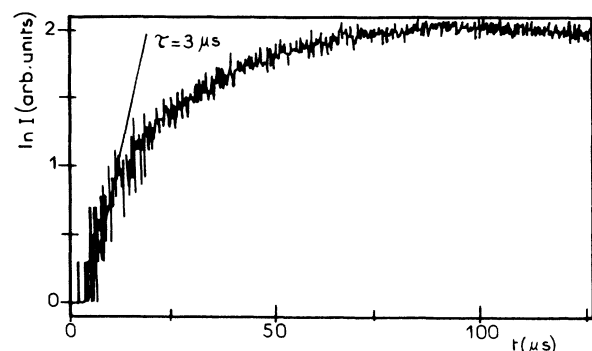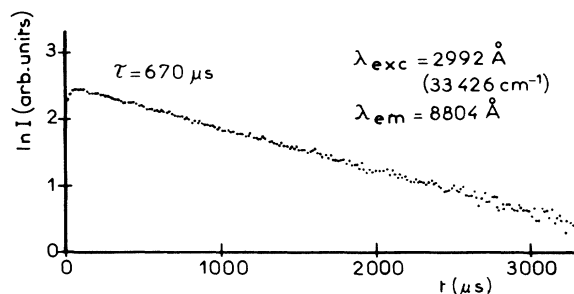
FIG. 6. Decay curves of the ir $^4F_{3/2}$ emission (in two different time scales) of LiYF$_4$: 0.1 at. % Nd^{3+} under one-photon pulsed excitation at 299.2 nm. $T = 4.4$ K. The points are the experimental data and the solid curve is their exponential fit.

FIG. 7. uv $^4D_{3/2}$ (358 nm) and blue $^2P_{3/2}$ (412 nm) fluorescence after 299.2 nm one-photon pulsed excitation of LiYF$_4$: Nd^{3+} at 4.4 K. The points are the experimental data and the solid curve is their exponential fit.

the case of the $^4I_{9/2}(1) \rightarrow {}^4G_{5/2}(1,2)$ transitions. The 0.17 cm^{-1} half-width of the $^4I_{9/2}(1) \rightarrow {}^4H(2)_{11/2}$ transition at 4.4 K is probably laser resolution limited; however, it indicates the low level of inhomogeneous broadening and a good crystal quality.

There is a large mean difference of about 30 cm^{-1} between the energy-level positions presented in Table II and the results reported by da Gama et al.[16] Our emission-line data are in good agreement with those of Fan and Byer[14] determined at 77 K for 2 at. % Nd^{3+} doped YLF. We paid special attention to the study of the high-energy Nd^{3+} levels, which participate in TPA or other stepwise processes. Precise absorption and excitation measurements at 4.4 K in the blue and uv region revealed much broader and less intense transitions than in the visible or ir. The lines are often associated with relatively intense vibronic sidebands, which largely complicates the analysis of spectra.

The two-photon excitation spectrum of the $^4D_{3/2}$ emission presented in Fig. 4 is composed of only one sharp line near 6038 Å (16 563 cm^{-1}). Its quadratic intensity dependence on the incident photon flux is characteristic of two-photon processes. The 6038 Å line intensity was found to be polarization independent. This, however, does not provide any important information because we have shown that the TPA of the $^4I_{9/2}(1) \rightarrow {}^2H(1)_{9/2}(i)$ transitions in S_4 symmetry are electric-dipole allowed for
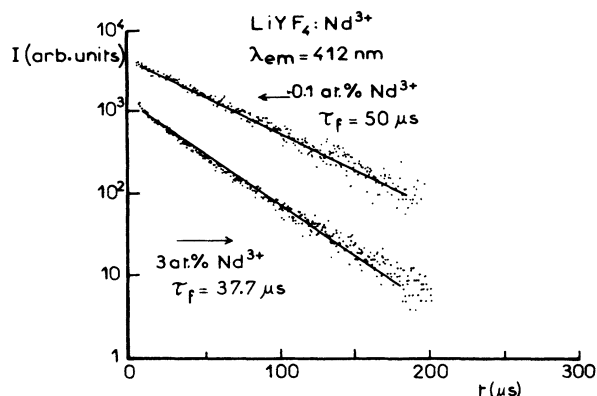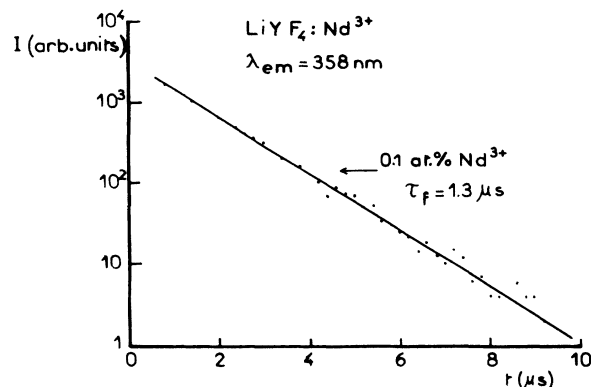
both σ and π polarizations; however, it is possible that the selection rules for the $^4F_{3/2} \rightarrow {}^4D_{3/2}$ transition determine the character of the observed transition. This, together with the results of our two-lasers two-photon experiments, indicates that some other mechanism is responsible for the anti-Stokes $^4D_{3/2}$ fluorescence. Because of the very low, 0.1 at. %, concentration of Nd^{3+} ions in the investigated system, the up-conversion energy transfer should not play a significant role.[20] Also, if this process was responsible for the creation of the $^4D_{3/2}$ population, then the excitation spectrum of the uv fluorescence would represent the ion-pair line spectrum as shown by Buisson et al.[12] This is, however, not the case and the observed uv signal arises after excitation of the absorption line center, as in the case of ir fluorescence (see Fig. 9).

This, together with the fact that the $^4D_{3/2}$ lifetime is independent of concentration, leaves the stepwise two-photon excitation as the only process responsible for the anti-Stokes fluorescence. Several possible energy combinations for two-photon resonances have been thoroughly investigated. It was found that the 16 563 cm^{-1} photon corresponds to the energy difference between the $^4D_{3/2}(1)$ and $^4F_{3/2}(1)$ levels. We also noted that the
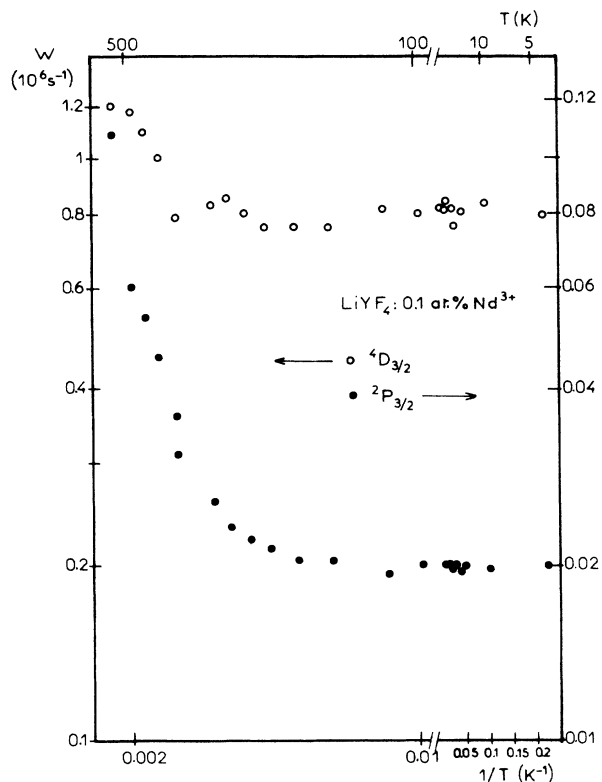
M. MALINOWSKI *et al.*

FIG. 8. $^4D_{3/2}$ and $^2P_{3/2}$ transition rates, $W = 1/\tau_f$, as a function of temperature in 0.1 at. % Nd^{3+} doped $LiYF_4$.
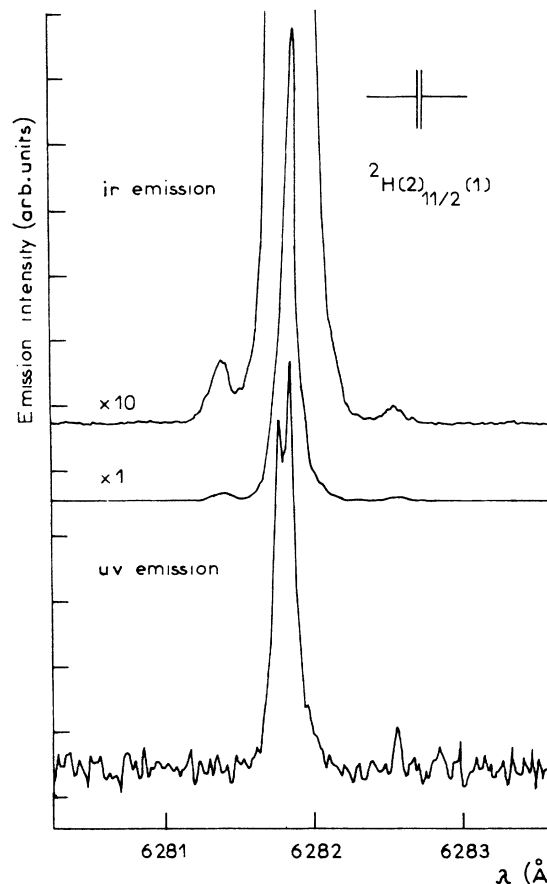

FIG. 9. High resolution excitation spectra of the uv and ir emission when the laser was scanned across the $^4I_{9/2}(1)$ $\rightarrow$ $^2H(2)_{11/2}(1)$ absorption transition of 0.1 at. % Nd^{3+} doped $LiYF_4$ at 4.4 K.
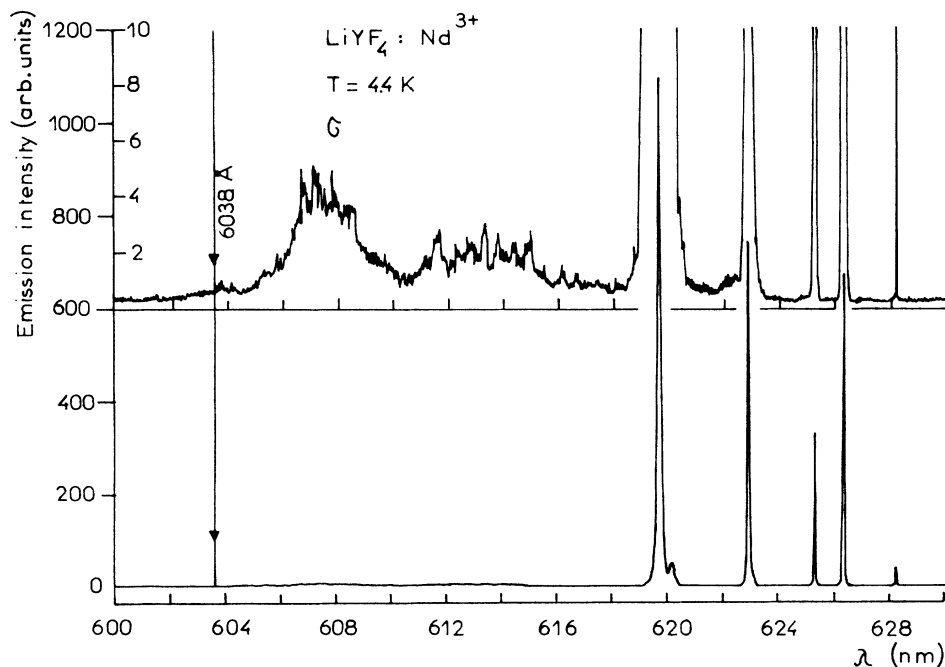

FIG. 10. Details of the vibronic band associated with the $^4I_{9/2}(1) \rightarrow$ $^2H(2)_{11/2}$ absorption transitions measured at 4.4 K. Position of the 603.8 nm excitation wavelength responsible for the anti-Stokes signal is indicated.

$^4I_{9/2}(1) \rightarrow {}^2H(2)_{11/2}$ transition is accompanied by a very weak vibronic sideband, which makes the nonresonant absorption of the $16\,563$ cm^{-1} photon possible (see Fig. 10). So the proposed model for stepwise uv excitation is as follows: the first $16\,563$ cm^{-1} photon is absorbed nonresonantly; this excitation relaxes to the lowest $^2H(2)_{11/2}$ level by very fast phonon emission, of the order of a few ns among the Stark levels; excitation then relaxes by a multistep process to a longer lived $^4F_{3/2}(1)$ state. The second $16\,563$ cm^{-1} photon reexcites resonantly the $^4D_{3/2}(1)$ level from this intermediate metastable state. The weak line around 6000 Å observed in the TP excitation spectrum in Fig. 4 is probably due to the $^4F_{3/2}(1) \rightarrow {}^4D_{3/2}(2)$ transition. Its weakness results from the decrease of the broad-band, one-photon absorption at wavelengths shorter than 6038 Å (see Fig. 10). There are also some features observed near 6008 Å; however, it is not possible at this time to explain their origin. Excited-state absorption (ESA) is also proposed to explain the $^4D_{3/2}(1)$ emission under resonant excitation of one of the $^2H(2)_{11/2}$ Stark levels. In this case any of the states excited by multi-step nonradiative decay to the lowest component of several lower-lying neodymium multiplets could participate as an intermediate metastable state in the second photon transition, which terminates on one of the high-energy states. Subsequent nonradiative relaxation then populates the $^4D_{3/2}(1)$ level. Some possible energy combinations for the ESA processes after resonant $^2H(2)_{11/2}(i)$-level excitation are given in Table III. In Fig. 11 the short wavelength absorption lines participating in the described ESA mechanism are shown. Energies corresponding to various processes listed in Table III are indicated.

It can be seen that several processes indicated in Fig. 11 (1, 2, 6, 10, 12, and 14) lead to quasiresonant excitation of the high-energy electronic levels of Nd^{3+}, namely $^4D_{5/2}$, $^4D_{1/2}$, $^2I_{11/2}$, and $^2L_{17/2}$ (see also Table III). These processes, together with various less-efficient transition terminating on the weak interline absorption, contribute in the $^4D_{3/2}$ excitation. From Table III it can also be seen that the $^4F_{5/2}(1)$ ESA at $12\,543$ cm^{-1} is mainly responsible for the uv signal under resonant $^2H(2)_{11/2}(i)$ excitation. The lifetime of the $^4F_{5/2}$ level was evaluated to be about 1.7 μs, (calculated from the nonradiative decay rate of 6×10^5 s^{-1} due to the 1000 cm^{-1} energy gap to the next lower level[21] and the radiative rate determined on the basis of Judd-Ofelt theory[22-24] to be 3.4×10^4 s^{-1}). This relatively long lifetime of the $^4F_{5/2}$ state favors the ESA process. However, it is also possible that, as shown by Macfarlane et al.[5] and Fan and Byer,[14] some upconversion by energy transfer could take place in more concentrated Nd^{3+} YLF crystals. The effective ESA cross section calculated in Ref. 14 was found to be 2×10^{-20} cm^2 at $^4G_{5/2}$ (5874 Å) π excitation in 2 at.% Nd^{3+} doped YLF. In our experiments we could expect the effective ESA cross section to be about 2 orders of magnitude smaller because of the lower population density of the $^4F_{5/2}$ excited state and expect the one-photon absorption coefficient for the $^4I_{9/2}(1) \rightarrow {}^2H(2)_{11/2}$ transitions to be lower by about a factor of 10. It is thus evident that it will be difficult to obtain laser action in the uv

TABLE III. Some possible energy combinations for two-photon resonances in the ESA process in LiYF$_4$: Nd^{3+}.

	Initial $^2H(2)_{11/2}$ level (cm^{-1})	Intermediate excited level (cm^{-1})	Final level (cm^{-1})	
1	15 919	15 919	31 838	$^2L_{17/2}$
2	15 919	14 747	30 666	$^2L_{17/2}$
3	15 919	13 492	29 411	$^2I_{11/2}$
4	15 919	12 534	28 453	$^4D_{5/2}$
5	15 967	14 747	30 714	$^2L_{17/2}$
6	15 967	12 534	28 501	$^4D_{5/2}$
7	15 995	15 919	31 914	$^2L_{17/2}$
8	15 995	14 747	30 742	$^2L_{17/2}$
9	15 995	13 492	29 487	$^2I_{11/2}$
10	15 995	12 534	28 529	$^4D_{5/2}$
11	16 055	14 747	30 802	$^2L_{17/2}$
12	16 055	12 534	28 589	$^4D_{5/2}$
13	16 126	14 747	30 873	$^2L_{17/2}$
14	16 138	14 747	30 885	$^2L_{17/2}$
15	16 138	12 534	28 672	$^4D_{5/2}$

or blue region in the present excitation configuration.

It is also interesting to note that there is a possibility of several radiative $^4D_{3/2}$ and $^2P_{3/2}$ transitions which are reabsorbed. These radiative processes could partly bypass the $^4F_{3/2}$ level but finally participate also in the creation of the $^4F_{3/2}$ population (but with time characteristics different from nonradiative processes). This mechanism could explain the slow buildup of the $^4F_{3/2}$ fluorescence presented in Fig. 6 where the observed 3 μs risetime could be related to the 1.3 μs radiative decay time of the $^4D_{3/2}$ level and slower decay of the $^2P_{3/2}$ state. This is also in agreement with the nearly quadratic dependence of the $^4F_{3/2}$ emission on the two 6038 Å photon excitation energy presented in Fig. 5. It could be sup-

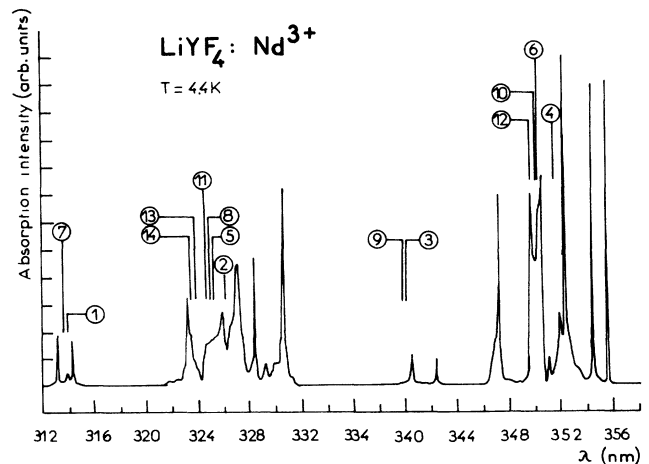FIG. 11. Short wavelength part of the 4.4 K LiYF$_4$: Nd^{3+} absorption spectrum. Final energies of various two-photon transitions discussed in the text and tabulated in Table III are indicated.
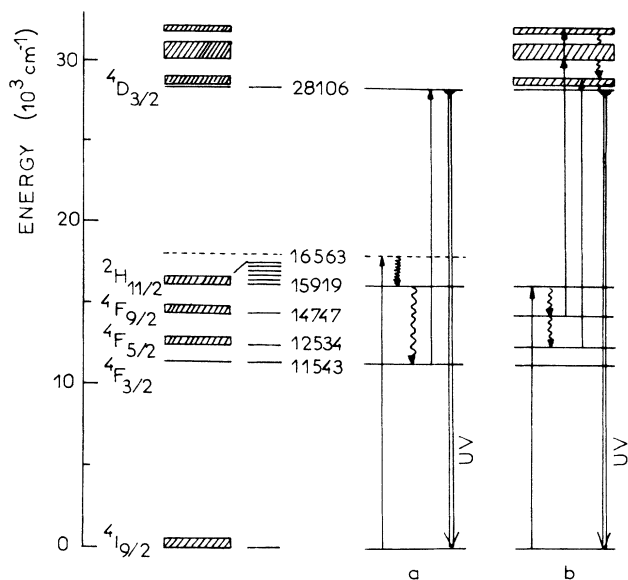
FIG. 12. Energy-level diagram of the Nd^{3+} ion in $LiYF_4$ showing excited state absorption processes discussed in the text. (Not all levels of Nd^{3+} are shown.)

posed that, in this case, the $^4F_{3/2}$ population is created mostly by the radiative transitions from the upper levels and that the rate of ESA is larger than the radiative $^4F_{3/2}$ emission probability.

On the basis of this analysis, and on intensity results, presented earlier, it is clear that several mechanisms are responsible for the creation of the excited-state popula-tion and that further one- and two-laser experiments are needed to determine its origin.

VI. CONCLUSIONS

The absorption and time-resolved (TR) excitation spectra of $LiYF_4:Nd^{3+}$ have been studied at 4.4 K and the detailed structure of high-energy Nd^{3+} levels was determined. The properties of the two metastable states, namely $^4D_{3/2}(1)$ at 28 106 cm^{-1} and $^2P_{3/2}(1)$ at 26 259 cm^{-1}, have been characterized under pulsed one photon excitation. The uv and blue fluorescences were also investigated after two-photon absorption. Several two-photon, two-laser excitations around the $^4I_{9/2}(1)$ $\rightarrow ^2H(2)_{11/2}(i)$ absorption transitions were performed. Two major quasiresonant excited-state absorption (ESA) processes from the $^4F_{3/2}(1)$ and the $^4F_{5/2}(1)$ and/or $^4F_{9/2}(1)$ levels were identified as responsible for the anti-Stokes $^4D_{3/2}(1)$ fluorescence.

*Permanent address: Institute of Microelectronics and Optoelectronics, P.W., ul. Koszykowa 75, Warsaw, Poland.

[1]V. S. Letokhov, in *Nonlinear laser chemistry, Multiple photon excitation,* edited by V. S. Letokhov and V. P. Chebotayev (Springer-Verlag, Berlin, 1983).

[2]M. Dagenais, M. Downer, R. Neuman, and N. Bloembergen, Phys. Rev. Lett. **46**, 561 (1981).

[3]C. D. Cordero-Montalvo and N. Bloembergen, Phys. Rev. B **30**, 438 (1984).

[4]A. J. Silversmith, W. Lenth, and R. M. Macfarlane, Appl. Phys. Lett. **51**, 1977 (1987).

[5]W. Lenth, A. J. Silversmith, and R. M. Macfarlane, in *Advances in Laser Science III,* edited by A. C. Tam, J. L. Gole, and W. C. Stwalley (American Institute of Physics, New York, 1988), p. 8.

[6]R. M. Macfarlane, T. Tong, A. J. Silversmith, and W. Lenth, Appl. Phys. Lett. **52**, 1300 (1988).

[7]H. G. Danielmeyer and M. Blatte, Appl. Phys. 1, 269 (1973).

[8]M. A. Kramer and R. W. Boyd, Phys. Rev. B **23**, 986 (1981).

[9]G. J. Quarles, G. E. Venikous, and R. C. Powell, Phys. Rev. B **31**, 6935 (1985).

[10]J. Mares, B. Jacquier, C. Pedrini, and G. Boulon, Mat. Chem. and Phys. **21**, 237 (1989).

[11]R. B. Barthem, J. C. Vial, and F. Madeore, J. Lumin. **34**, 47 (1985).

[12]R. Buisson, J. Q. Liu, and J. C. Vial, J. Phys. (Paris) **45**, 1533 (1984).

[13]L. L. Chase and S. A. Payne, Phys. Rev. B **34**, 8883 (1986).

[14]T. Y. Fan and R. L. Byer, J. Opt. Soc. Am. B **3**, 1519 (1986).

[15]R. M. Macfarlane (unpublished).

[16]A. A. S. da Gama, G. F. de Sá, P. Porcher, and P. Caro, J. Chem. Phys. 75, 2583 (1981).

[17]J. D. Axe, Jr., Phys. Rev. A **42**, 136 (1964).

[18]R. B. Barthem, R. Buisson, J. C. Vial, and H. Harmand, J. Lumin. **34**, 295 (1986).

[19]D. Curie, *Champ Cristallin et Luminescence* (Gauthier-Villars, Paris, 1968).

[20]A. L. Harmer, A. Linz, and D. R. Gabbe, J. Phys. Chem. Solids **30**, 1483 (1969).

[21]B. R. Reddy and P. Vankateswalu, J. Chem. Phys. **79**, 5845 (1983).

[22]H. P. Jenssen, Crystal Physics Laboratory Technical Report No. 16, MIT Cambridge Mass., 1971 (unpublished), p. 83.

[23]B. R. Judd, Phys. Rev. **127**, 750 (1962).

[24]G. S. Ofelt J. Chem. Phys. **37**, 311 (1962).